

Decay process of the Mg 2p core exciton in magnesium halides studied by photoelectron spectroscopy

Osamu Aita, Kouichi Ichikawa, and Kenjiro Tsutsumi

College of Engineering, University of Osaka Prefecture, Mozu, Sakai, Osaka 591, Japan

(Received 12 October 1988)

The decay of the Mg 2p core exciton in MgF₂, MgCl₂, and MgBr₂ was investigated by use of the technique of resonant photoemission. The constant-initial-state (CIS) spectrum with the initial state at the peak of the valence band and the constant-final-state (CFS) spectrum with the final state corresponding to the kinetic energy of the Auger electron were measured at photon energies around the Mg 2p core-exciton excitation in these substances. The resonant enhancements were observed in the CIS and CFS spectra of MgCl₂ and MgBr₂, whereas in MgF₂ only the Auger-electron peak shows resonant behavior. These resonant enhancements are interpreted in terms of the nonradiative decay of the Mg 2p core exciton through the $L_{2,3}(\text{exciton})-V$ and the $L_{2,3}(\text{exciton})-VV$ processes, respectively, where $L(\text{exciton})$ denotes the initial state with the L hole accompanied by a bound electron (L core exciton) and V denotes the final state with a hole in the valence band. The shapes of the valence-band energy distribution curves obtained at the photon energies of the L_2 and the L_3 core-exciton excitations are different in MgCl₂ and MgBr₂. This is attributed to the difference in the relaxation of the L_2 and the L_3 core excitons.

I. INTRODUCTION

The decay mechanism of the core exciton in alkali halides has been investigated by several groups.¹⁻¹³ We investigated the nonradiative decay process of the Li 1s core exciton in lithium halides⁷⁻⁹ and also of the Na 2p core exciton in sodium halides¹⁰⁻¹³ by using the experimental technique of resonant photoemission first introduced by Lapeyre *et al.*¹ We observed resonant enhancement in the constant-initial-state (CIS) spectrum with the initial state at the peak of the valence band and in the constant-final-state (CFS) spectrum with the final state corresponding to the kinetic energy of the Auger electron, and proposed the following two decay processes of the core exciton: (1) a core hole and a photoexcited electron that form the core exciton recombine directly with energy transferred to a valence electron, and (2) the core hole forming a core exciton recombines with a valence electron, transferring energy to another valence electron which is excited to the continuum. The former process is called the $K(\text{exciton})-V$ process in lithium halides or the $L_{2,3}(\text{exciton})-V$ process in sodium halides, where $K(\text{exciton})$ or $L_{2,3}(\text{exciton})$ denotes the initial state with the K hole or the $L_{2,3}$ hole accompanied by a bound electron (K core exciton or $L_{2,3}$ core exciton¹⁴), and V denotes the final state with a hole in the valence band. The latter process is called the $K(\text{exciton})-VV$ process in lithium halides or the $L_{2,3}(\text{exciton})-VV$ process in sodium halides. The kinetic energy of the Auger electron is slightly greater than that of the ordinary Auger electron because in the final state of this decay process two valence holes and one electron can be attracted to one another to result in a bound state.^{7,8,10}

In the previous study we found two peaks in the CIS and CFS spectra of NaCl and NaBr.¹¹⁻¹³ The intense

peak on the higher-energy side coincides in energy with the L_2 core-exciton peak in the respective absorption spectra, but the lower-energy peak does not coincide in its shape and in energy with the L_3 core-exciton peak in the respective absorption spectra. Moreover, the lower-energy peak shows the strong dependence on the incident angle of the polarized light on the sample surface,¹² but does not show the clear dependence on temperature.¹³ Since the photoelectron spectrum of sodium halides suffers the surface effect owing to the short mean free path of the photoelectrons (about 8–20 Å) obtained at the photon energy of the Na 2p core-exciton excitation,¹⁵ and the evaporated films used for that study had a surface with strong preferred orientations which were $\langle 100 \rangle$ and $\langle 110 \rangle$ for NaCl and $\langle 100 \rangle$ and $\langle 111 \rangle$ for NaBr, the lower-energy peak was assigned as the peak due to the surface core exciton. Moreover, the dependence of this peak on the incident angle of the polarized light was interpreted as being due to two kinds of surface core excitons, which are formed in the crystal field of the C_{4v} symmetry at the surface,^{12,13,16} excited with the parallel and the perpendicular components of the electric field vector of the polarized light to the sample surface.^{12,13} On the other hand, the higher-energy peak in the CIS and CFS spectra of NaCl and NaBr shows no remarkable change in its shape and in excitation energy as a function of the incident angle of the photon beam. This feature in the CIS and CFS spectra also shows temperature dependence similar to that of the L_2 core-exciton peak in the absorption spectrum. Thus this higher-energy peak was attributed to the decay peak of the ordinary bulk L_2 core exciton. The surface core exciton is usually observed on the lower-energy side of the bulk core exciton with an energy difference of a few tenths of an eV, which is accidentally comparable to the spin-orbit splitting of the Na 2p level.

Since the L_3 core-exciton peak is less intense than the L_2 core-exciton peak in the absorption spectra, the decay of the bulk L_3 core exciton was not clearly observed in the CIS and CFS spectra, owing to the overlap of the decay peak of the surface core exciton.

The optical properties of magnesium halides were investigated by several authors¹⁷⁻²² and the peaks observed in the Mg $L_{2,3}$ absorption spectra were ascribed to the core excitons.¹⁸ The purpose of the present study is to study the characteristics of the decay processes of the bulk L_2 and the bulk L_3 core excitons in magnesium halides with less disturbance by the surface core exciton, because the mean free path of the photoelectrons in magnesium halides in this energy region is longer than that in sodium halides.²³ Besides, even if structures due to the surface core exciton appear, they would be weak and complicated and would not be distinguishable as clear peaks since the surface structure of evaporated films of magnesium halides is very complicated.

II. EXPERIMENT

Photoelectron spectra were measured at room temperature (RT) and liquid-nitrogen temperature (LNT) by using an ultrahigh-vacuum photoelectron spectrometer with a 2-m grazing-incidence monochromator of a modified Rowland-mount type. Synchrotron radiation from a 400-MeV electron storage ring at the Institute for Solid State Physics of the University of Tokyo was used as a light source. The spectral width was about 0.1 eV at the photon energy of 54 eV with 100- μ m entrance and 50- μ m exit slits and a 1200-groove/mm grating. The energy of the photoelectrons was measured with a double-stage electrostatic electron-energy analyzer of the cylindrical mirror type. The analyzer resolution was constant with a full width at half maximum (FWHM) of 0.4 eV. The angle between the incident photon beam and the ejected electron (the entrance axis of the electron-energy analyzer) was fixed. The incident angle of the photon beam on the sample surface was at first set at 0°. In this case the electric field vector of incident photons is parallel to the sample surface. Subsequently the incident angle was set at 45° so that the angle between the electric field vector of incident photons and the sample surface was the same as in the previous experiments on sodium halides.^{11,12}

Since charging of the sample may result in a shift and a broadening of the structure in the photoelectron spectrum, samples with a thickness of about 100 Å were prepared *in situ* by evaporation onto gold substrates. MgI₂ was not investigated because this substance decomposed during the evaporation. The base pressure in the sample chamber was about 3×10^{-8} Pa and rose to the 10^{-6} -Pa range during the evaporation. The pressure in the analyzer chamber was 4×10^{-9} Pa during measurements. The spectral dependence of the radiation incident on the samples was determined from the photoelectric yield spectrum of gold.

The absorption spectra were measured by using synchrotron radiation from a 750-MeV electron storage ring at the Institute for Molecular Science. A plane-grating

monochromator equipped with a Ni-coated cylindrical focusing mirror and a Pt-coated toroidal refocusing mirror was used for the present measurement. The spectral width was about 0.1 eV at the photon energy of 54 eV with a 1200-groove/mm grating and a 100- μ m exit slit, which is almost the same as that of the monochromator used for the measurement of the photoelectron spectra. The prefilter made of aluminum film was used to suppress higher-order light from the grating below 70 eV. Absorption films were prepared *in situ* by evaporation onto collodion substrates coated with a thin aluminum film. The pressure in the sample chamber was about 10^{-5} Pa during the evaporation and dropped immediately to 10^{-7} Pa after the evaporation. To obtain the absorption coefficients, the thickness of the samples was measured with an oscillating-quartz thickness gauge calibrated by Tolansky interferometry.

III. RESULTS AND DISCUSSION

A. Decay of the Mg 2p core exciton

Figures 1–3 show sets of energy distribution curves (EDC's) of photoelectrons for MgF₂, MgCl₂, and MgBr₂, respectively, which were obtained at various photon energies around the Mg 2p core-exciton excitation. These EDC's were obtained at RT with an incident angle of 45°. The excitation photon energies are given on the right-

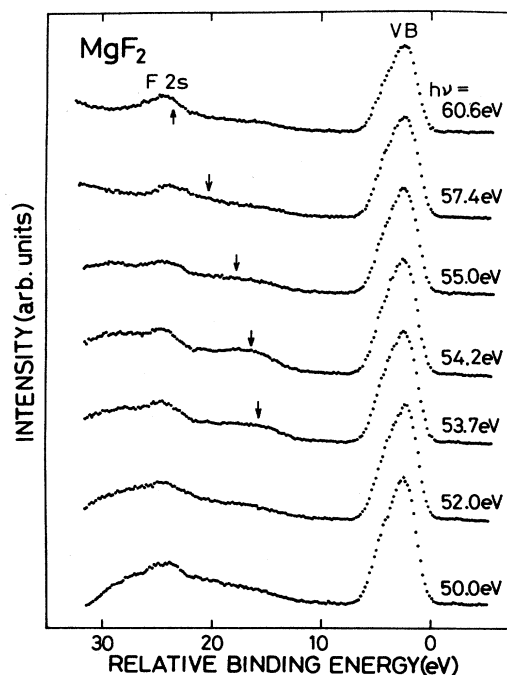


FIG. 1. Set of EDC's of MgF₂ obtained at photon energies around the Mg 2p core-exciton excitation. These spectra were measured at RT with the incident angle of 45°. Intensities are normalized to the incident photon flux. The Auger-electron peaks are indicated by arrows.

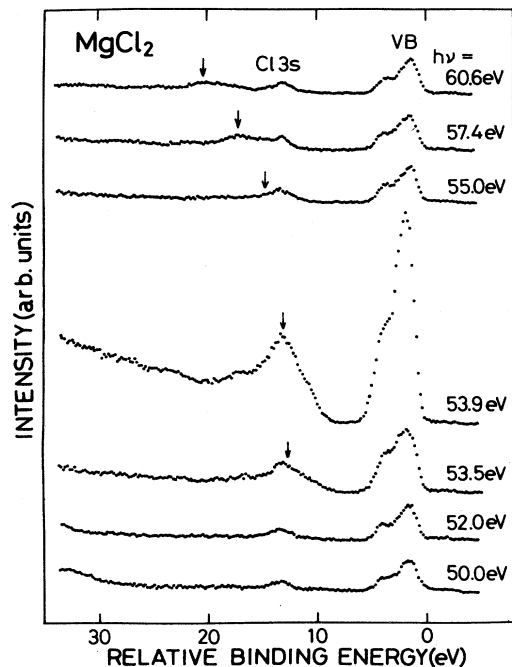


FIG. 2. Set of EDC's of MgCl_2 obtained at photon energies around the $\text{Mg } 2p$ core-exciton excitation. These spectra were measured at RT with the incident angle of 45° . Intensities are normalized to the incident photon flux. The Auger-electron peaks are indicated by arrows.

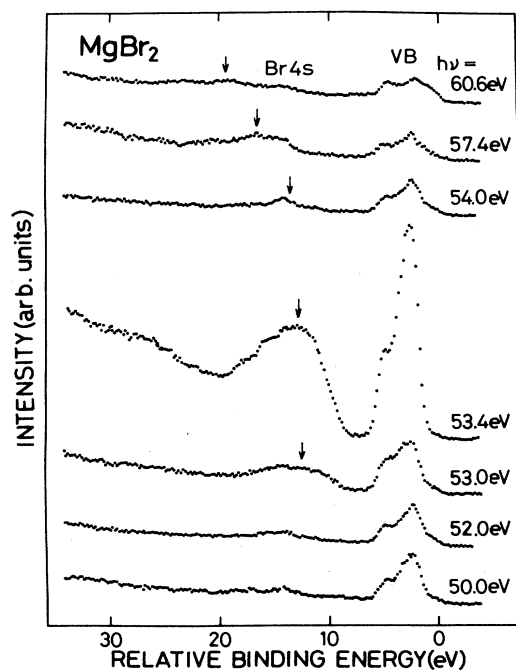


FIG. 3. Set of EDC's of MgBr_2 obtained at photon energies around the $\text{Mg } 2p$ core-exciton excitation. These spectra were measured at RT with the incident angle of 45° . Intensities are normalized to the incident photon flux. The Auger-electron peaks are indicated by arrows.

hand side of each spectrum. The binding energies are given relative to the top of the valence band. The ordinate is proportional to the number of photoelectrons per incident photon flux.

The valence-band EDC's of MgF_2 show a single peak, whereas those of MgCl_2 and MgBr_2 consist of a main peak and a peak on its higher-binding-energy side. The binding energies of these peaks are listed in Table I, together with those of the outermost s levels of the anions and the $\text{Mg } 2p$ levels. The valence-band EDC's of MgCl_2 and MgBr_2 are resonantly enhanced at the photon energies of the $\text{Mg } 2p$ core-exciton excitation, whereas the valence-band EDC's of MgF_2 do not show such an enhancement. It is noticed that the valence-band EDC's of MgCl_2 and MgBr_2 are different in shape with the change of photon energies around the core-exciton excitation.

The Auger-electron peak, which is shown by arrows in Figs. 1–3, is observed in every case when the excitation photon energy is greater than about 53 eV. This result indicates that the Auger decay process of the $\text{Mg } 2p$ hole state occurs before the ionization threshold of the $\text{Mg } 2p$ electron (the threshold energy from the $\text{Mg } 2p$ level to the conduction band is about 55 eV), and suggests that the $\text{Mg } 2p$ hole produced by the formation of the $\text{Mg } 2p$ core exciton (the excitation energy is about 53 eV) decays through the Auger process [the $L_{2,3}(\text{exciton})-VV$ process]. The Auger-electron peak is also enhanced at the photon energies of the $\text{Mg } 2p$ core-exciton excitation in all the magnesium halides studied. The kinetic energy of the ordinary Auger electron excited at photon energies greater than the threshold energy of the $\text{Mg } 2p$ level is also listed in Table I. The kinetic energy is represented with respect to the top of the valence band for convenience.

These resonant phenomena are more visual in the CIS spectra with the initial state at the peak of the valence band and in the CFS spectra with the final state corresponding to the kinetic energy of the Auger electron. The CIS and CFS spectra obtained at RT with the incident angle of 45° are shown in Figs. 4–6 together with the $\text{Mg } L_{2,3}$ absorption spectra. The absorption coefficient is given on the right-hand side of the figure. The CFS spectra show the resonant behavior at 54.19 eV in MgF_2 , at 53.44 and 53.87 eV in MgCl_2 , and at 52.97

TABLE I. The binding energies of valence band, outermost s level of the anion, and $\text{Mg } 2p$ level, and the kinetic energies of the ordinary Auger electrons. Energies are given relative to the top of the valence band in electron volts.

	MgF_2	MgCl_2	MgBr_2
Valence band			
peak	2.5	2.0	3.1
shoulder		4.0	5.5
full width	6.7	5.6	7.1
Anion ns level	24.2	13.2	15.9
$\text{Mg } 2p$ level	45.4	48.2	51.4
FWHM	1.8	1.2	1.1
$L_{2,3}-VV$	36.9	40.1	40.0

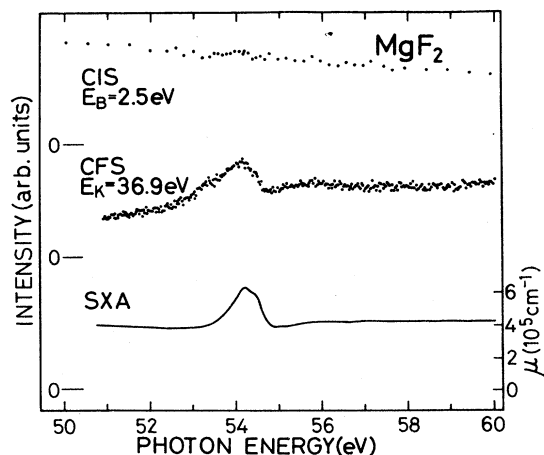


FIG. 4. CIS spectrum measured at the initial binding energy of 2.5 eV, CFS spectrum with the final kinetic energy of 36.9 eV, and the Mg $L_{2,3}$ absorption spectrum of MgF_2 . These spectra were measured at RT.

and 53.37 eV in $MgBr_2$. The energy positions of these peaks in the CFS spectra agree well with those of the Mg 2p core-exciton peaks observed in the absorption spectra (54.17 eV in MgF_2 , 53.44 and 53.86 eV in $MgCl_2$, and 52.93 and 53.36 eV in $MgBr_2$). The FWHM values of the peaks in the CFS spectra of $MgCl_2$ and $MgBr_2$ are in good agreement with those of the exciton peaks in the absorption spectra, whereas the FWHM value of the peak in the CFS spectrum of MgF_2 is greater than that of the exciton peak in the absorption spectrum.

The CIS spectrum of MgF_2 does not show remarkable enhancement in the excitation-photon-energy range shown in Fig. 4 compared with the case of the other magnesium halides. This feature is similar to the case of the Na L_2 core exciton in NaF, in which the CIS spectrum showed the dip rather than the enhanced peak. We inter-

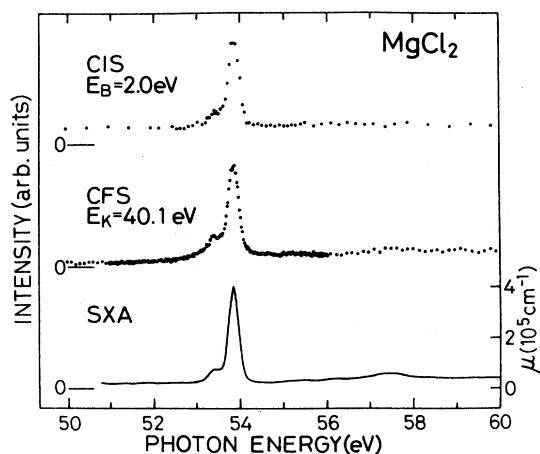


FIG. 5. CIS spectrum measured at the initial binding energy of 2.0 eV, CFS spectrum with the final kinetic energy of 40.1 eV, and the Mg $L_{2,3}$ absorption spectrum of $MgCl_2$. These spectra were measured at RT.

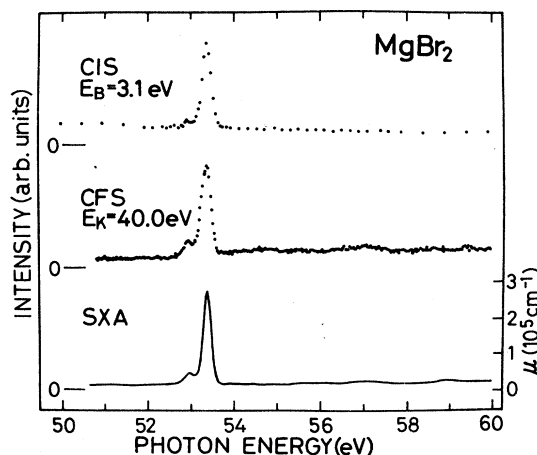


FIG. 6. CIS spectrum measured at the initial binding energy of 3.1 eV, CFS spectrum with the final kinetic energy of 40.0 eV, and the Mg $L_{2,3}$ absorption spectrum of $MgBr_2$. These spectra were measured at RT.

preted it as being due to the anomalies of the escape function of the photoelectron and the reflectivity of the incident photon on the sample surface.^{10,13} Though similar consideration may be available for the case of MgF_2 , detailed analysis is necessary in the future.

On the other hand, a prominent peak and a small peak are observed in the CIS spectra at 53.89 and 53.45 eV in $MgCl_2$ and at 53.37 and 52.92 eV in $MgBr_2$, respectively. The energy positions of these peaks coincide well with those of the peaks in the respective absorption spectra. The shape of the CIS spectra is in agreement with those of the absorption and CFS spectra as seen in Figs. 5 and 6.

The energy positions of the main peak and its lower-energy peak in the CIS and CFS spectra of $MgCl_2$ and $MgBr_2$ coincide well with the respective exciton peaks in the absorption spectra which show the bulk properties. The CIS, CFS, and absorption spectra resemble one another except for the slight difference in the intensity ratio of the lower-energy peak to the main peak among these spectra. In addition, no clear dependence of the spectral shape on the incident angle of the photon beam was obtained in the CIS and CFS spectra of magnesium halides. Thus the main peak and the lower-energy peak in the CIS and CFS spectra are ascribed to the decay peak due to the bulk L_2 and the bulk L_3 core excitons, respectively.

Upon cooling the sample to LNT, the main peak and the lower-energy peak shift to the higher-energy side by the same amount as the energy shift of the respective peaks due to the bulk L_2 and the bulk L_3 core excitons in the absorption spectrum, and their widths become narrower, like those of the core-exciton peaks in the absorption spectrum. As an example, the CIS and CFS spectra of $MgCl_2$ measured at RT and LNT with the incident angle of 0° are shown in Fig. 7 together with the absorption spectra. In this figure solid and dashed lines represent the spectra obtained at LNT and RT, respectively. This

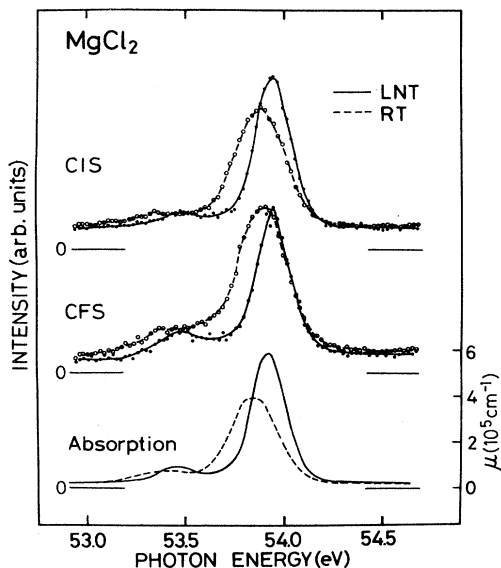


FIG. 7. CIS and CFS spectra of MgCl_2 measured at RT (dashed lines) and LNT (solid lines) with the incident angle of 0° . The $\text{Mg } L_{2,3}$ absorption spectra measured at RT and LNT are also shown in the bottom.

temperature dependence is further evidence that the lower-energy peak, as well as the main peak, in the CIS and CFS spectra is due to the bulk core exciton and not due to the surface core exciton. Peaks due to the surface core excitons, which were observed in sodium halides, were not clearly observed in magnesium halides as expected from the reason mentioned in Sec. I.

From the resonant behavior in the CIS and CFS spectra one infers that the bulk L_2 and the bulk L_3 core excitons in magnesium halides decay through the $L_{2,3}(\text{exciton})-V$ and the $L_{2,3}(\text{exciton})-VV$ processes. However, the $\text{Mg } 2p$ core exciton in MgF_2 does not decay noticeably through the $L_{2,3}(\text{exciton})-V$ process.

B. Energy shift of the Auger-electron peak through the $L_{2,3}(\text{exciton})-VV$ process

We investigated the energy shift of the Auger-electron peak in the $L_{2,3}(\text{exciton})-VV$ process of the $\text{Mg } 2p$ core exciton. To determine the energy position of the Auger-electron peak, we subtracted the components due to the outermost s level of the anion, the valence band, and its secondary electrons from the raw photoelectron spectra. The Auger-electron spectra of MgCl_2 thus obtained are shown in Fig. 8 for various excitation photon energies. When the excitation photon energy is around the energy of the core exciton, the kinetic energy of the Auger-electron peak shifts to the greater kinetic energy side of the ordinary $L-VV$ Auger-electron peak obtained at a photon energy far from resonance. The dependence of the kinetic energy of the Auger electron on the excitation photon energy could not be obtained for MgBr_2 because the additional peaks due to the secondary electrons or the photoelectrons excited from the $\text{Br } 4d$ level by the

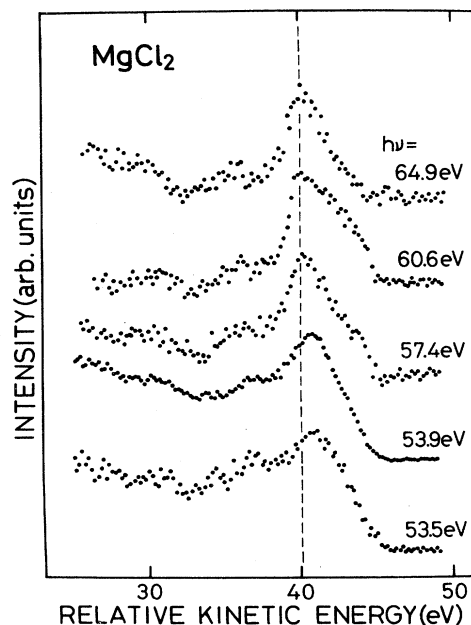


FIG. 8. Auger-electron spectra derived by the subtraction of the valence band, its secondary electrons, and the $\text{Cl } 3s$ band from the raw photoelectron spectra. The dashed line shows the energy position of the Auger-electron peak appearing in the raw photoelectron spectrum measured at the photon energy of 69.8 eV. The intensity of the Auger-electron peak is normalized at the peak.

second-order light (with a photon energy twice as much as the first-order photon energy) appear in the spectra. Since the Auger-electron peak shows a broad peak, it was difficult to distinguish the peak due to the $L_3(\text{exciton})-VV$ process from that due to the $L_2(\text{exciton})-VV$ process. Figure 9 shows the results of the peak positions of the Auger electron for (a) MgF_2 and (b) MgCl_2 . The ordinate in this figure indicates the increment of the kinetic energy ΔE_K from that of the ordinary $L_{2,3}-VV$ Auger electron. The arrows indicate the thresholds for the transition from the $\text{Mg } 2p$ level to the conduction band obtained from the binding energies of the $\text{Mg } 2p$ level given in Table I and the band-gap data.^{20,21} As seen in this figure, the kinetic energy of the Auger electron in the $L_{2,3}(\text{exciton})-VV$ process is greater by 0.5–0.8 eV than that of the ordinary $L_{2,3}-VV$ Auger electron in MgF_2 and MgCl_2 .

Energy shifts of the Auger-electron peak were interpreted as the effect of postcollision interaction (PCI) in inner-shell ionization in some gaseous and solid materials.^{24,25} In the case of the PCI, the Coulomb repulsion between a slow photoelectron receding from the atom and a fast Auger electron emitted in the decay of that atom can produce an upward shift of the kinetic energy of the observed Auger electron. It was reported that the shift of the Auger-electron peak due to the PCI is about 0.3 eV at the ionization threshold of the core level,²⁴ and is still observed with the excitation energies up to several hundreds of electron volts above the threshold.²⁶ In the present case, the upward energy shift of the Auger-

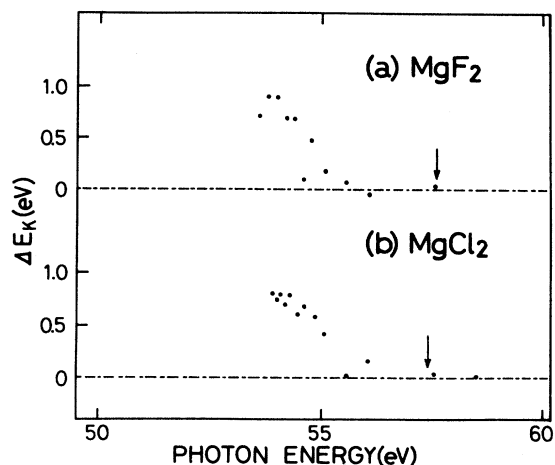


FIG. 9. Peak positions of the main Auger peak of (a) MgF₂ and (b) MgCl₂ as a function of photon energy. Ordinate indicates the increment of the kinetic energy from that of the ordinary $L_{2,3}$ -VV Auger peak. Arrows indicate the thresholds for the transition from the Mg 2p level to the conduction band which were obtained from the band-gap energies (Refs. 20 and 21) and the binding energies of the Mg 2p levels measured in the present study.

electron peak is observed when the photon energy is below the excitation energy of the Mg 2p electron to the bottom of the conduction band. When the Mg 2p core exciton decays through the $L_{2,3}$ (exciton)-VV process, the final state consists of the two holes in the valence band, one electron in the bound state, and one electron in the continuum state. Therefore, it is considered that the correlation energy among two holes and a bound electron in the final state plays an important role in the present case.

The three-body problem including two valence holes and a single conduction electron, which appears in the study of the final state of the resonant photoemission in insulators and semiconductors, has been theoretically investigated by Igarashi.²⁷ According to his result, the kinetic energy of the Auger electron increases from that of the ordinary Auger electron when the photon energy is near the excitation energy of the core exciton and this energy shift is related to the formation of the trion state (the two-holes-and-one-electron bound state). Recently Watanabe, Kuramoto, and Kato calculated the binding energy of the trion state to be 0.4–0.8 eV in lithium halides.²⁸ This binding energy is close to the increment of the kinetic energy of the Auger electron observed around the excitation photon energies of the core excitons in lithium halides,⁸ sodium halides,¹⁰ and the present case of magnesium halides. Thus, the energy shift of the Auger-electron peak may be interpreted by the formation of the trion state in the final state of the $L_{2,3}$ (exciton)-VV process.

C. Decay probability of the Mg 2p core exciton

Previously, we estimated the nonradiative decay probabilities of the Li 1s core exciton in lithium halides⁸ and

the Na 2p core exciton in sodium halides.¹⁰ In a similar manner we estimated the decay probability of the Mg 2p core exciton in magnesium halides through the $L_{2,3}$ (exciton)-V and the $L_{2,3}$ (exciton)-VV processes. The decay probability P through the $L_{2,3}$ (exciton)-V process is given by the equation^{8,10}

$$P = \frac{I_{\text{ex}}/I_{\text{VB}}}{\mu_{\text{ex}}/\mu_{\text{VB}}}, \quad (1)$$

where I_{ex} and I_{VB} are the area of the enhanced part of the valence-band EDC obtained at the photon energy of the core-exciton excitation and the integrated intensity of the valence-band EDC obtained at a photon energy far from resonance, respectively. The quantities μ_{ex} and μ_{VB} are the parts of the absorption coefficient due to the creation of the core exciton and due to the excitation of the valence electron at the photon energy of the core-exciton excitation, respectively. The ratio $\mu_{\text{ex}}/\mu_{\text{VB}}$ was derived from the EDC obtained at the photon energy of the EDC spectrum, under the assumption that the ratio of the integrated intensity of the valence-band EDC to that of the outermost s level of the anion observed in the photoelectron spectrum is the same as the ratio of the absorption coefficients μ_{VB}/μ_s at the photon energy of the core-exciton excitation, where μ_s is the part of the absorption coefficient due to the electronic transition from the outermost s level. The decay probability P' through the $L_{2,3}$ (exciton)-VV process is expressed as follows:^{8,10}

$$P' = P \frac{S_{\text{Aug}}}{S_{\text{VB}}}. \quad (2)$$

Here, S_{Aug} and S_{VB} are the integrated intensity of the Auger peaks due to the $L_{2,3}$ (exciton)-VV process and the increase of the valence-band intensity due to the $L_{2,3}$ (exciton)-V process at the photon energy of the core-exciton excitation. The decay probabilities of the Mg 2p core exciton through the $L_{2,3}$ (exciton)-V and $L_{2,3}$ (exciton)-V processes are shown in Table II.

The decay probabilities of the L_2 (exciton)-V and the L_3 (exciton)-V processes are almost the same in the respective materials and those of the L_2 (exciton)-VV and the L_3 (exciton)-VV processes are also nearly the same in the respective materials. The decay probabilities of the Mg 2p core exciton through the L_2 (exciton)-V and the L_3 (exciton)-V processes increase in going from chloride to bromide. Since the ionicity of these substances decreases in going from MgCl₂ to MgBr₂,²⁹ the delocalization of the valence-band wave function in magnesium halides seems to play an important role in the decay

TABLE II. Decay probabilities of the Mg 2p core exciton through the $L_{2,3}$ (exciton)-V and the $L_{2,3}$ (exciton)-VV processes.

	MgF ₂		MgCl ₂		MgBr ₂	
	L_2	L_3	L_2	L_3	L_2	L_3
L (exciton)-V			0.20	0.20	0.26	0.29
L (exciton)-VV			0.10	0.12	0.24	0.30

probability of the core excitons as the decay probability of the Na L_2 core exciton in sodium halides.

It is noted that the decay probability through the $L_{2,3}(\text{exciton})-VV$ process is comparable to or less than that of the $L_{2,3}(\text{exciton})-V$ process in magnesium halides. This result is contrary to the cases of lithium halides and sodium halides in which the decay probability through the $K(\text{exciton})-VV$ process in lithium halides or the $L_2(\text{exciton})-VV$ process in sodium halides is greater than that through the $K(\text{exciton})-V$ process or the $L_2(\text{exciton})-V$ process, respectively.

D. Valence-band EDC's measured at the photon energies of the core-exciton excitation

The shape of the valence-band EDC's of MgCl_2 and MgBr_2 changes drastically with the change of the excitation photon energy around the core-exciton excitation. The valence-band EDC's of MgCl_2 measured at the photon energies of the L_2 core-exciton excitation (53.9 eV), the L_3 core-exciton excitation (53.5 eV), and 56.0 eV (off resonance) are shown by solid, dashed, and dotted lines in Fig. 10(a), respectively. Those of MgBr_2 measured at the photon energies of the L_2 core-exciton excitation (53.4 eV), the L_3 core-exciton excitation (53.0 eV), and 56.0 eV

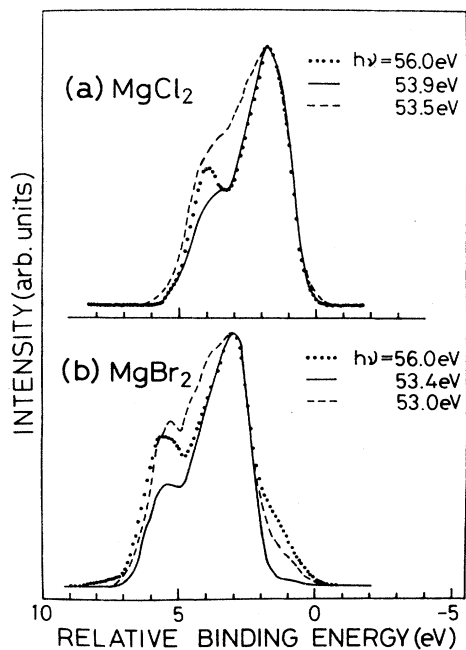


FIG. 10. (a) Comparison of the valence-band EDC's of MgCl_2 . Dotted, solid, and dashed lines indicate the EDC's obtained at 56.0 eV, 53.9 eV (L_2 core-exciton excitation), and 53.5 eV (L_3 core-exciton excitation), respectively. (b) Comparison of the valence-band EDC's of MgBr_2 . Dotted, solid, and dashed lines indicate the EDC's obtained at 56.0 eV, 53.4 eV (L_2 core-exciton excitation), and 53.0 eV (L_3 core-exciton excitation), respectively. Intensities are normalized at the peak in the respective figures.

(off resonance) are also shown by solid, dashed, and dotted lines in Fig. 10(b), respectively. These spectra are normalized at the peak. As seen in these figures, in the valence-band EDC measured at the photon energy of the L_2 core-exciton excitation the main peak is more enhanced than other parts of the valence band, whereas the part in the higher-binding-energy region of the main peak is more enhanced in the valence-band EDC measured at the photon energy of the L_3 core-exciton excitation.

In the decay process of the Li 1s core exciton in lithium halides it was proposed that the probability of the excitation of each valence electron due to the $K(\text{exciton})-V$ process is not the same as that due to the direct photoexcitation, and electrons existing at some singular points in the valence band are selectively excited by the annihilation of the core exciton.⁹ The width of the valence-band EDC's of MgCl_2 and MgBr_2 observed at the photon energy of the L_2 core-exciton excitation is narrower than that obtained at a photon energy far from resonance. This suggests that the particular states are more enhanced than the other states in the valence band in the decay of the Mg 2p core exciton through the $L_{2,3}(\text{exciton})-V$ process.

However, the part in the higher-binding-energy region of the main peak in the valence-band EDC obtained at the photon energy of the L_3 core-exciton excitation is broader and more enhanced than that obtained at a photon energy far from resonance. This difference in the enhancement of the valence-band EDC's between the $L_2(\text{exciton})-V$ and the $L_3(\text{exciton})-V$ processes is interpreted as being due to the difference in the relaxation of the core exciton under the nonequilibrium condition. This mechanism was proposed in the case of the annihilation of the Li 1s core exciton in lithium halides, owing to the interaction between the electron system and the lattice system. By the Franck-Condon principle, the optical excitation transfers an electron from the ground state in equilibrium into a nonequilibrium excited state. Then, the exciton thus formed in a nonequilibrium condition relaxes into the equilibrium excited state through the interaction between the exciton and the lattice. As a result of this relaxation, the energy transferred to the valence electron through the $L_3(\text{exciton})-V$ process under this condition is reduced from the energy necessary to create the L_3 core exciton. Because the system might relax while reaching equilibrium, the energy transferred to the valence electron during the annihilation of the core exciton is equal to, or less than, the creation energy of the core exciton. This gives rise to the broadening of the enhanced profile of the valence-band EDC due to the $L_3(\text{exciton})-V$ process to the higher-binding-energy side. That is, the L_3 core exciton may suffer the interaction with the crystal lattice and cause the relaxation with phonon emission to bring the system into thermal equilibrium during the annihilation of the core exciton.

This consideration is supported by the fact that the FWHM value of the peak due to the L_3 core exciton in the absorption spectra is wider than that due to the L_2 core exciton. That is, the FWHM values of the L_2 and

the L_3 core-exciton peaks in the absorption spectrum of MgCl_2 are 0.27 and 0.32 eV, respectively, and those of MgBr_2 are 0.23 and 0.32 eV, respectively. According to Toyozawa,³⁰ the FWHM value of the absorption peak due to the exciton is a measure of the strength of the electron-lattice coupling in the exciton system. In fact, the width of the absorption peaks due to the L_2 and the L_3 core excitons in MgCl_2 and MgBr_2 becomes narrower upon cooling the sample to LNT. The reason why the electron-lattice interaction is different between the L_2 and the L_3 core excitons is not clear yet, but it should be noticed that the exciton state relating to the excitation of the Mg 2p electron should be treated with the intermediate coupling scheme, as remarked in Ref. 14. According to Onodera and Toyozawa,³¹ the exchange interaction between the electron and the hole mixes two exciton states of $(\frac{3}{2}, \frac{1}{2})$ and $(\frac{1}{2}, \frac{1}{2})$, where the first number in the parentheses indicates the total angular momentum j of the hole and the second specifies j of the electron. The coupling would produce an admixture of states different from those produced by the spin-orbit interaction only. This admixture gives rise to changes in the intensity ratio and the doublet splitting from the expected values for the $(\frac{3}{2}, \frac{1}{2})$ and $(\frac{1}{2}, \frac{1}{2})$ excitons. It would give rise to a difference in the electron-lattice coupling, causing the difference in the extent of the relaxation between the L_2 and the L_3 core excitons. As a consequence of this difference in relaxation, one observes the resonant enhancement of the valence-band EDC's at a binding energy greater than that of the main peak.

Moreover, there is a possibility that the electrons in the different states in the valence band are selectively excited by the annihilation of the L_2 and the L_3 core excitons, because the core-exciton wave function describing the L_2 and the L_3 core excitons is modified by the coupling between the exciton state and that of the valence electron. However, to assure this situation it is necessary to calculate the matrix elements describing the overlap between the exciton system and the valence state in the many-electron system.

IV. CONCLUSION

The decay of the Mg 2p core exciton in MgF_2 , MgCl_2 , and MgBr_2 was investigated by photoelectron spectroscopy with synchrotron radiation. It was observed that the intensities of the valence-band EDC and the Auger-electron peak are resonantly enhanced at the photon energies of the Mg 2p core-exciton excitation in MgCl_2 and MgBr_2 , whereas in MgF_2 only the Auger-electron peak shows resonant behavior. These resonant enhancements

are interpreted in terms of the nonradiative decay of the Mg 2p core exciton through the $L_{2,3}(\text{exciton})-V$ and the $L_{2,3}(\text{exciton})-VV$ processes. The correlation between two holes and one electron in the final state of the core-exciton decay through the $L_{2,3}(\text{exciton})-VV$ process, which was suggested in the cases of lithium halides^{7,8} and sodium halides,¹⁰ was confirmed by the energy shift of the Auger-electron peak in magnesium halides.

In MgCl_2 and MgBr_2 the energy positions and the shapes of the peaks in the CIS and CFS spectra are almost the same as those of the bulk L_2 and the bulk L_3 core excitons in the absorption spectrum. Upon cooling the sample to LNT these peaks shift to the higher-energy side by the same amount as the energy shift of the respective core-exciton peaks in the absorption spectra measured at LNT. Also, these spectra did not show any dependence on the incident angle of the polarized light on the sample surface. Thus the peaks observed in the CIS and CFS spectra of magnesium halides are ascribed to the decay of the bulk L_2 and the bulk L_3 core excitons.

The decay probability of the Mg 2p core exciton through the $L_2(\text{exciton})-V$ and the $L_3(\text{exciton})-V$ processes increases in going from chloride to bromide, and thus, it was found that the delocalization of the valence-band wave function seems to play an important role in the decay process of the Mg 2p core exciton in magnesium halides. The decay probabilities of the $L_2(\text{exciton})-V$ and the $L_3(\text{exciton})-V$ processes are almost the same in the respective materials and the decay probability of the $L_{2,3}(\text{exciton})-VV$ process is also nearly the same between the L_2 and the L_3 core excitons in the respective materials.

The shape of the valence-band EDC of MgCl_2 and MgBr_2 was found to change drastically with the change of the excitation photon energy around the core-exciton excitation. To interpret this change, it was proposed that the relaxation of the L_3 core exciton occurs during its decay through the $L_3(\text{exciton})-V$ process but the L_2 core exciton does not suffer this type of remarkable relaxation.

ACKNOWLEDGMENTS

The authors are grateful to the staff of the Synchrotron Radiation Laboratory of the Institute for Solid State Physics of the University of Tokyo, and also to the staff of the Ultraviolet Synchrotron Orbital Radiation Facility of the Institute for Molecular Science, for their assistance during experiments. This work was supported in part by a Grant-in-Aid for Scientific Research from the Ministry of Education, Science and Culture, Japan.

¹G. J. Lapeyre, A. D. Baer, J. Harmanson, J. Anderson, J. A. Knapp, and P. L. Gobby, *Solid State Commun.* **15**, 1602 (1974).

²E. T. Arakawa and M. W. Williams, *Phys. Rev. Lett.* **36**, 333 (1976).

³O. Aita, K. Tsutsumi, K. Ichikawa, M. Kamada, M. Okusawa,

H. Nakamura, and T. Watanabe, *Phys. Rev. B* **23**, 5676 (1981).

⁴J. H. Beaumont, A. J. Bourdillon, and M. N. Kabler, *J. Phys. C* **9**, 2961 (1976).

⁵R. Haensel, G. Keitel, G. Peters, P. Schreiber, B. Sonntag, and C. Kunz, *Phys. Rev. Lett.* **23**, 530 (1969).

- ⁶H. Sugawara and T. Sasaki, *J. Phys. Soc. Jpn.* **46**, 132 (1979).
- ⁷M. Kamada, K. Ichikawa, and K. Tsutsumi, *Phys. Rev. B* **28**, 7225 (1983).
- ⁸K. Ichikawa, M. Kamada, O. Aita, and K. Tsutsumi, *Phys. Rev. B* **32**, 8293 (1985).
- ⁹K. Ichikawa, M. Kamada, O. Aita, and K. Tsutsumi, *Phys. Rev. B* **34**, 1227 (1986).
- ¹⁰M. Kamada, O. Aita, K. Ichikawa, and K. Tsutsumi, *Phys. Rev. B* **36**, 4962 (1987).
- ¹¹K. Tsutsumi, O. Aita, and K. Ichikawa, *J. Phys. (Paris) Colloq.* **48**, C9-919 (1987).
- ¹²O. Aita, K. Ichikawa, and K. Tsutsumi, *Phys. Rev. B* **38**, 10079 (1988).
- ¹³K. Ichikawa, O. Aita, and K. Tsutsumi, *Phys. Rev. B* **39**, 1307 (1989).
- ¹⁴The core exciton in the Mg $L_{2,3}$ absorption spectra of magnesium halides should be treated with the intermediate coupling scheme, since the energy of the exchange interaction between an electron and a hole of the core exciton and the spin-orbit splitting of the Mg $2p$ level are comparable in magnesium halides. In the present case, however, we use the nomenclature in the usual spectroscopic notation for simplicity.
- ¹⁵F. L. Battye, J. Liesegang, R. C. G. Leckey, and J. G. Jenkin, *Phys. Rev. B* **13**, 2646 (1976).
- ¹⁶U. Rehder, W. Gudat, R. G. Hayes, and C. Kunz, in *Proceedings of the 7th International Vacuum Congress and the 3rd International Conference on Solid Surfaces*, edited by R. Dobrozemsky, F. Rüdener, F. P. Viehböck, and A. Breth (Berger, Vienna, 1977), p. 453.
- ¹⁷W. F. Hanson, E. T. Arakawa, and M. W. Williams, *J. Appl. Phys.* **43**, 1661 (1972).
- ¹⁸P. Rabe, B. Sonntag, T. Sagawa, and R. Haensel, *Phys. Status Solidi B* **50**, 559 (1972).
- ¹⁹M. Scrocco, *Phys. Rev. B* **33**, 7228 (1986).
- ²⁰G. Stephan, Y. Le Calvez, J. C. Lemonier, and S. Robin, *J. Phys. Chem. Solids* **30**, 601 (1969).
- ²¹S. Kinno and R. Onaka, *J. Phys. Soc. Jpn.* **49**, 1379 (1980).
- ²²S. Kinno and R. Onaka, *J. Phys. Soc. Jpn.* **50**, 2073 (1981).
- ²³G. E. McGuire and P. H. Holloway, in *Electron Spectroscopy: Theory, Techniques, and Applications*, edited by C. R. Brundle and A. D. Baker (Academic, London, 1981), Vol. 4, p. 7.
- ²⁴V. Schmidt, S. Krummacher, F. Wuilleumier, and P. Dhez, *Phys. Rev. A* **24**, 1803 (1981).
- ²⁵T. Miller and T.-C. Chiang, *Phys. Rev. B* **29**, 1121 (1984).
- ²⁶S. Ohtani, H. Nishimura, H. Suzuki, and K. Wakiya, *Phys. Rev. Lett.* **36**, 863 (1976).
- ²⁷J. Igarashi, *J. Phys. Soc. Jpn.* **54**, 2762 (1985).
- ²⁸T. Watanabe, Y. Kuramoto, and H. Kato (private communication).
- ²⁹L. Pauling, *The Nature of the Chemical Bond*, 3rd ed. (Cornell University Press, Ithaca, 1960), p. 99.
- ³⁰Y. Toyozawa, *Prog. Theor. Phys.* **20**, 53 (1958).
- ³¹Y. Onodera and Y. Toyozawa, *J. Phys. Soc. Jpn.* **22**, 833 (1967).